Development and Evaluation of the PRIME Plume Rise and Building Downwash Model

Article *in* Journal of the Air & Waste Management Association (1995) · April 2000

DOI: 10.1080/10473289.2000.10464017 · Source: PubMed

3 authors, including:

Lloyd Schulman
Exponent
25 PUBLICATIONS **446** CITATIONS

SEE PROFILE

Journal of the Air & Waste Management Association (in press)

DEVELOPMENT AND EVALUATION OF THE PRIME PLUME RISE AND BUILDING DOWNWASH MODEL

Lloyd L. Schulman

David G. Strimaitis

Joseph S. Scire

Earth Tech, Inc., 196 Baker Avenue, Concord, MA USA 01742

ABSTRACT

A new Gaussian dispersion model, PRIME, has been developed for plume rise and building downwash. PRIME considers the position of the stack relative to the building, streamline deflection near the building, and vertical wind speed shear and velocity deficit effects on plume rise. Within the wake created by a sharp-edged, rectangular building, PRIME explicitly calculates fields of turbulence intensity, wind speed, and streamline slope, which gradually decay to ambient values downwind of the building. The plume trajectory within these modified fields is estimated using a numerical plume rise model. A probability density function and an eddy diffusivity scheme are used for dispersion in the wake. A cavity module calculates the fraction of plume mass captured by and recirculated within the near wake. The captured plume is re-emitted to the far wake as a volume source and added to the uncaptured primary plume contribution to obtain the far wake concentrations. The modeling procedures currently recommended by the U.S. Environmental Protection Agency, using SCREEN and the Industrial Source Complex model (ISC), do not include these features. PRIME also avoids the discontinuities resulting from the different downwash modules within the current models and the reported over predictions during light wind speed, stable conditions. PRIME is intended for use in regulatory models. PRIME was evaluated using data from a power plant measurement program, a tracer field study for a combustion turbine, and several wind-tunnel studies. PRIME performed as well as, or better than ISC/SCREEN for nearly all of the comparisons.

INTRODUCTION

The entrainment of exhaust gases released by short stacks or rooftop vents into the wakes of buildings can result in ground-level pollutant concentrations that are significantly larger than those from gases released at the same height in the absence of the buildings. The concentrations are dependent upon the complex airflow patterns near the buildings as well as the stack location and the characteristics of the exhaust gases. The influence of buildings on plume dispersion has been the subject of many wind-tunnel studies and some field studies, mostly for non-buoyant plumes from stacks on the roof or in the immediate lee of isolated buildings during neutral, moderate to high wind speed conditions. A number of mathematical formulas and models have also been proposed to simulate aerodynamic building downwash. Comprehensive reviews of many of these studies and models are available in Hosker[1] and Meroney[2].

Current Environmental Protection Agency (EPA) recommendations for modeling building downwash are divided into two categories: (1) the SCREEN3 model (U.S. EPA[3]) is recommended for receptors in the near-wake (the recirculation cavity downwind of the building), and (2) the Industrial Source Complex (ISC) model (U.S. EPA[4]) is recommended for receptors in the far-wake and beyond. The SCREEN model downwash algorithm uses a wake height formulation from Hosker[1] that, because of insufficient data, did not depend on the ratio of building width to height. This omission, plus the restriction that either all or none of the plume is captured by the cavity, was shown by Schulman and Scire[5] to lead to unrealistically large predicted concentrations for many narrow buildings (width and length less than height) and unrealistically small or zero predicted concentrations for many squat buildings (width and length greater than height.)

The ISC downwash model was constructed by EPA as a combination of two algorithms. The first, based on Huber and Snyder[6], is applied for stacks taller than 1.5 times the building height. The second, based on Scire and Schulman[7] and Schulman and Hanna[8], is applied for shorter stacks. These downwash algorithms have several important limitations: (1) the location of the stack relative to the building is not considered (if the stack is determined to be within the general region of influence of the building, the stack is always treated as though it were at the center of the lee wall of the building); (2) streamline deflection is not considered (ascent of the mean streamlines upwind of and over the building and descent in the lee of buildings); (3) effects of

in-wake turbulence intensity and wind speed on plume rise are not included; (4) the concentrations are not linked to any plume material that may have been captured by the near wake; (5) there are discontinuities at the interface between the two separate downwash algorithms used in ISC; (6) there are no wind direction effects for squat buildings; (7) large concentrations predicted during light wind speed, stable conditions are not supported by observations.

A new model, the **P**lume **Ri**se **M**odel **E**nhancements (PRIME) model has been developed to incorporate the two fundamental features associated with building downwash: enhanced plume dispersion coefficients due to the turbulent wake, and reduced plume rise caused by a combination of the descending streamlines in the lee of the building and the increased entrainment in the wake. The PRIME algorithms (Version 99020) have been integrated into the ISC model, and can be installed in other analytical, Gaussian-based models.

This paper summarizes some of the data used to develop PRIME, presents the formulation of the new model, and compares the model predictions with field and wind-tunnel observations.

WIND-TUNNEL AND FIELD DATA

A significant portion of the PRIME development effort was directed towards measuring flow fields and plume behavior near buildings, which provided valuable data for model development. (A separate, independent evaluation was conducted after the completion of the model (EPRI [9]).) Fluid modeling simulations were conducted at the EPA Meteorological Wind Tunnel (Snyder[10] and Snyder and Lawson[11]). These simulations provided concentration and flow field measurements for several generic building and source configurations. Some of the findings from these studies were presented by Snyder[12] and Snyder and Lawson [13]. In Snyder[12], descent of the mean streamlines above and downwind of a steam boiler building was noted. The largest ground-level concentrations were observed for a stack located just downwind of the building. For stacks located upwind of the building, the plume was released in a region of ascending streamlines and plume rise was higher than for stacks located downwind of the building. As the stack was moved farther downwind of the building, the ground level concentrations decreased. Figure 1, taken from Snyder and Lawson[13], illustrates streamline deflection for flow perpendicular to a cubic building. It was also observed that plumes from shorter stacks released in the region of strong

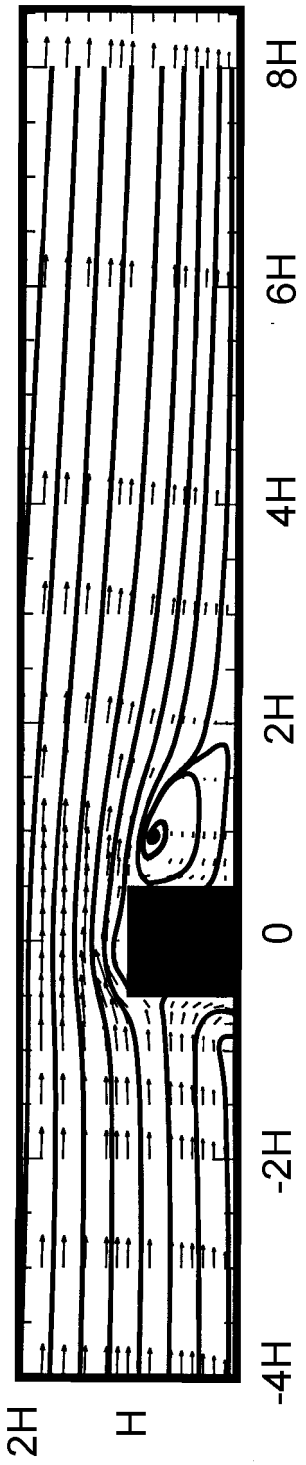

Figure 1. Vertical cross section of wind-tunnel simulation of streamlines near a cubic building. Vertical and horizontal axes are number of building heights, H. (Adopted from Snyder and Lawson[13]).

shear and turbulence near the ground resulted in lower rise than that experienced by plumes released from taller stacks. That rise was initially higher for plumes released just downwind of the building, where winds speeds were lower than in the absence of the building. Fluid modeling was also conducted at the Monash University Wind Tunnel (Melbourne and Taylor[14]). Simulations were conducted for two full-scale facilities; the Lee Power Plant in North Carolina and the Sayreville Generating Station in New Jersey. The Sayreville site was also the location of the project field study. The wind-tunnel simulations were used to confirm and extend the field results from a combustion turbine plume at the plant.

The field study at the Sayreville Generating Station was conducted from 10 February to 5 March 1994. Four instrumented, 10m towers were deployed and measurements of wind speed and direction, wind turbulence, temperature, humidity, and short-wave and long-wave radiation were made (Oncley[15]). A mobile, 1.06 micron wavelength Mark IX lidar system (Kaiser, et al.[16]) collected back scatter data from the particulate plumes released by both a combustion turbine and a steam boiler with short stacks. These data were processed to obtain one hour average centroid and variances for the composite plume images. The steam boiler building had a crosswind dimension about twice its height. The stack was located on the building and rose to a height 40% higher than the building's roof. The primary combustion turbine building had a crosswind dimension of just over half its height, with the exhaust vent flush with its roof.

The steam boiler plume was observed to descend downwind of the boiler house during two high wind speed events (Scire, Schulman and Strimaitis[17]). The slope of the descent was greatest on the day when the wind was oriented nearly 45 degrees to the face of the steam boiler building, instead of perpendicular to the building. The wind speed and boiler operation were nearly identical on both days. The plume rise from the combustion turbine was too high above the turbine roof to be significantly affected by the descending flow induced by nearby structures.

In addition to the wind-tunnel and field data, three-dimensional numerical modeling, using a finite element turbulence model, was conducted to provide a numerical laboratory for other building shapes and orientations. Comparisons of the numerical model simulations with the wind-tunnel observations showed similar velocity vectors, but a larger recirculation zone (Brzoska, Stock and Lamb[18]).

FORMULATION OF THE PRIME MODEL

The wind-tunnel and field studies made clear that incorporating estimates of wind speed, streamline deflection, and turbulence intensities in the wake, as well as including the location of the source relative to the building, were crucial to improving modeling simulations of the influence of buildings on ground-level concentrations. This is the central approach used in PRIME; to explicitly treat the trajectory of the plume near the building, and to use the position of the plume relative to the building to calculate interactions with the building wake. PRIME calculates fields of turbulence intensity, wind speed, and the slopes of the mean streamlines as a function of projected building shape. These fields gradually decay to ambient values downwind of the building. Using a numerical plume rise model, PRIME determines the change in plume centerline location and the rate of plume dispersion with downwind distance in these fields. Plume rise incorporates the advection along mean streamlines, and rise of the plume relative to the streamlines due to buoyancy and momentum. Concentrations are predicted in both near and far wakes, with the plume mass captured by the near wake treated separately from the uncaptured primary plume, and re–emitted to the far wake as a volume source. Figure 2 presents a schematic of the downwash process for two plumes illustrating the importance of stack location.

Cavity and Wake Dimensions

The building cavity is defined as the region bounded above the roof by the separation streamline originating at the upwind roof edge, and bounded downwind of the building by the reattachment streamline. The cavity is bounded laterally by the streamlines separating from the corners. Depending on the building geometry, there can be distinct roof-top and downwind cavities, or a single recirculation cavity. The cavity downwind of the building is often called the near-wake or separation bubble. The wake beyond the reattachment streamline is called the far wake. A wake envelope bounds the recirculation cavities and the far wake. These wake features are unsteady. A schematic of the building wake is shown in Figure 3. Simple formulae for height and width of the cavity envelope ($H_c(x)$, $W_c(x)$) and the wake boundary ($H_w(x)$, $W_w(x)$) are defined below.

The structure of the cavity and wake is controlled by the building dimensions, as projected along-wind and crosswind. These dimensions are the building height (H), the projected building width across the flow (W), and the projected building length along the flow (L). Following Wilson[19], a length scale for flow and diffusion near a building is defined as,

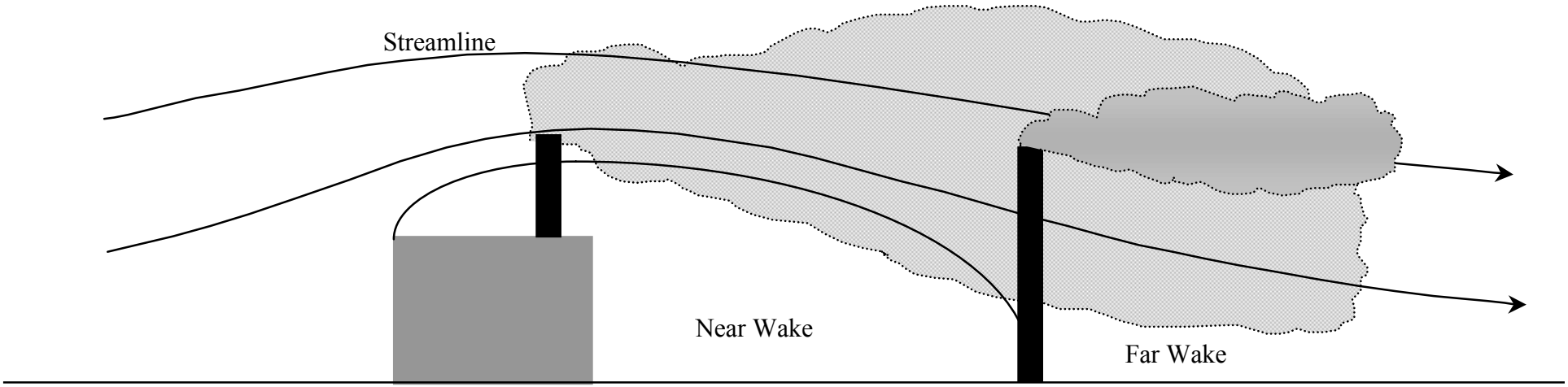

Figure 2. Schematic of building downwash for two identical plumes emitted at different locations. The plume released from the rooftop stack has a larger rate of growth and more descent than the plume released farther downwind.

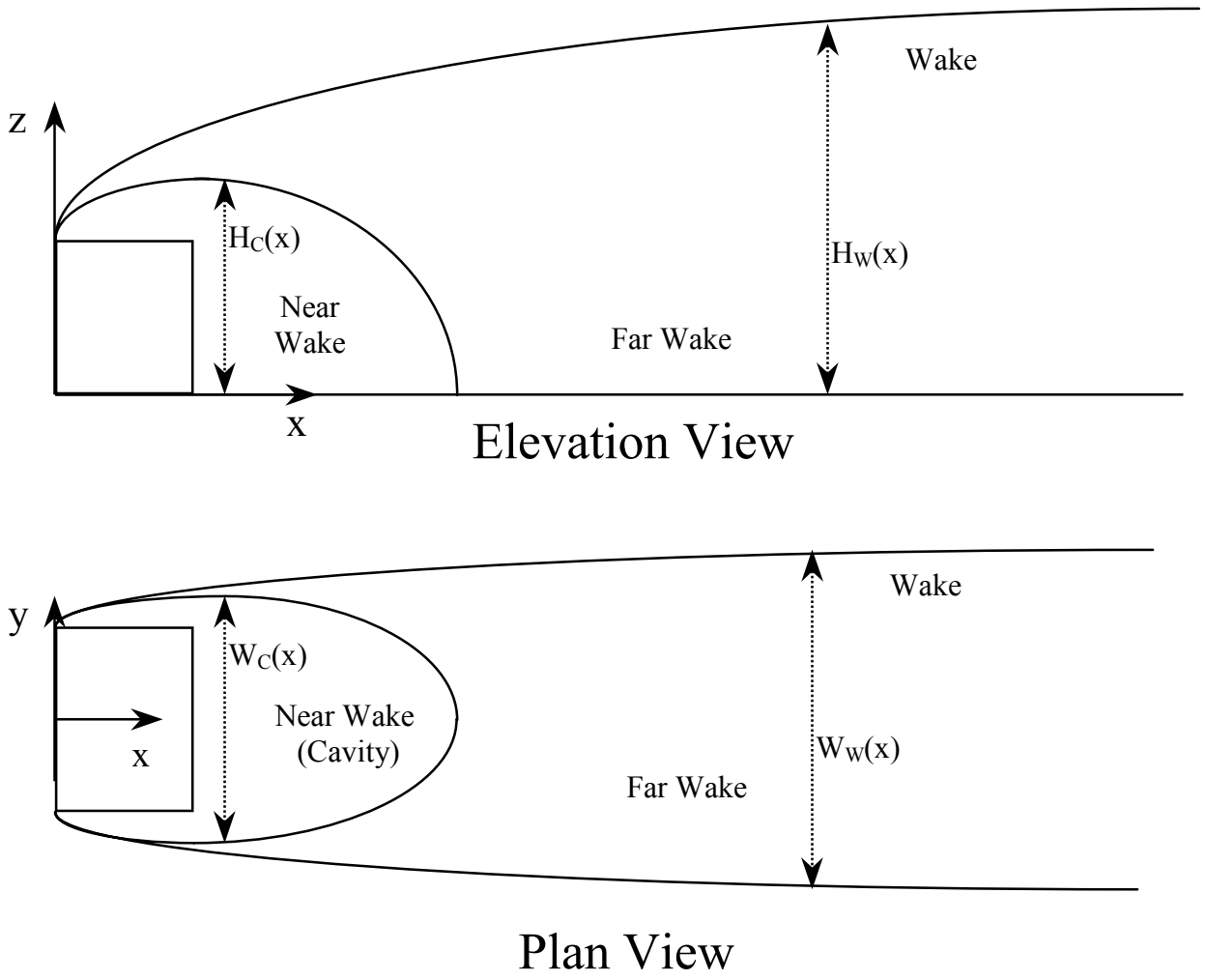

Figure 3. Schematic of building wake for the elevation view (top) and plan view (bottom). x denotes downwind distance, z the height, and y the cross wind distance. The wake boundary grows as $x^{1/3}$ both vertically and horizontally.

$$R = B_S^{2/3} B_L^{1/3} \tag{1}$$

where B_S is the smaller and B_L is the larger of H and W. The value used for B_L is capped at $8B_S$ (ASHRAE[20]). The roof-top cavity will reattach to the building if L > 0.9R (Wilson[19]). If the roof-top cavity reattaches to the building, the maximum height of the downwind recirculation cavity (Wilson and Britter[21]) is $H_R = H$. If the roof-top cavity does not reattach, the maximum height of the downwind cavity (Wilson[19]) is $H_R = H + 0.22R$ at x = 0.5R, where x is the along-wind distance measured from the upwind face of the building. The length of the downwind recirculation cavity, measured from the lee face of the building, is estimated by Fackrell [22] as,

$$L_R = \frac{1.8W}{\left[(L/H)^{0.3} (1.0 + 0.24W/H) \right]} \qquad (0.3 \le L/H \le 3.0) \tag{2}$$

When the ratio L/H lies outside the indicated range, L_R is computed using the nearer limit. Cavity lengths computed from Equation (2) are compared with the distances to the mean streamline reattachment points determined from wind-tunnel velocity measurements (Snyder and Lawson[13]) for ten different building shapes in Figure 4. Five of these buildings had W=H and L/H values ranging from near zero (a fence) to 4. The remaining shapes had W=L and H/W values from 1 to 3.

Using R, L_R, and H_R, ellipse segments are used to calculate the height and width of the cavity envelope as a function of along-wind distance from the upwind face of the building ($H_c(x)$, $W_c(x)$). If the rooftop cavity reattaches to the building, the envelope height is calculated as,

$$H_C = H \qquad (0 < x \le L) \tag{3}$$

$$H_C = H\left[1 - \left(\frac{x - L}{L_R} \right)^2 \right] \qquad (L > x > L + L_R) \tag{4}$$

If the cavity does not reattach to the building,

$$H_C = H_R + \frac{4\left(x - \frac{R}{2} \right)^2 (H - H_R)}{R^2} \qquad (0 < x \le R/2) \tag{5}$$

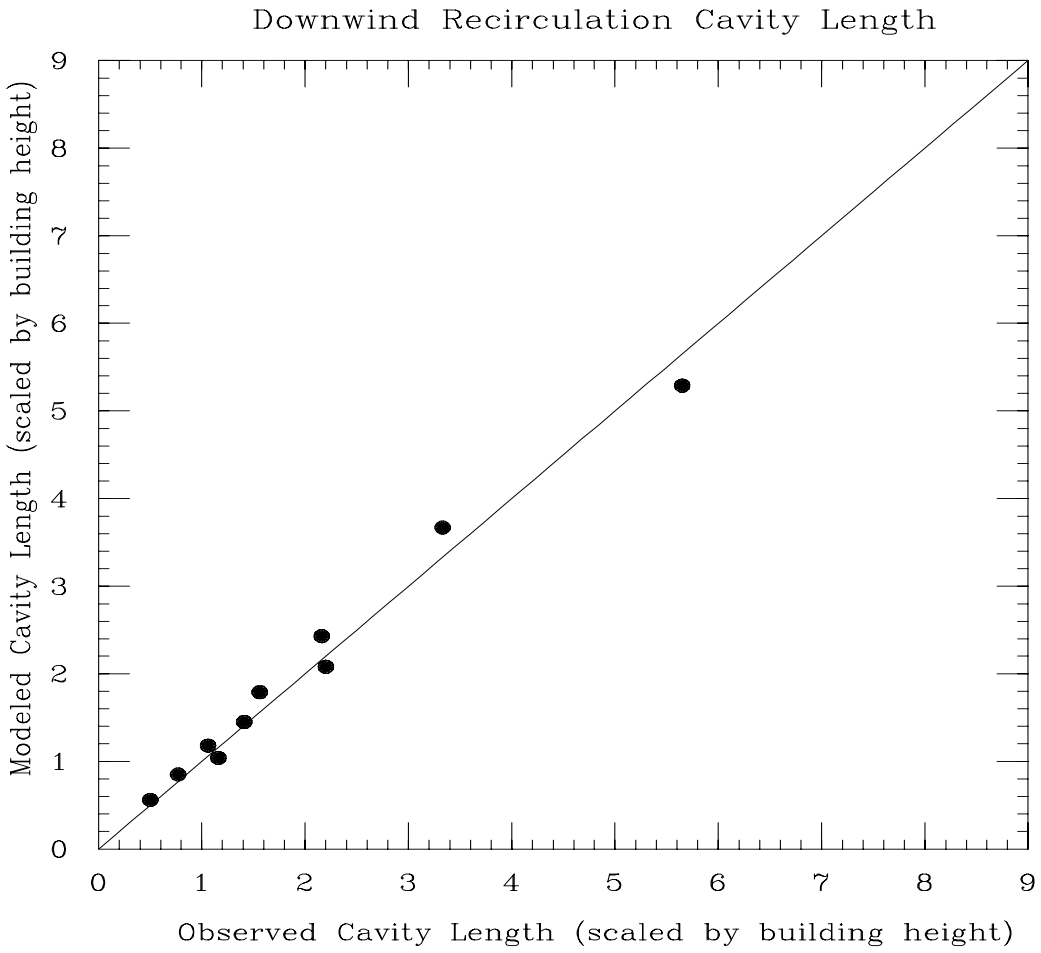

Figure 4. Comparison of the lengths of the downwind recirculation cavities for ten different building shapes as calculated by the PRIME model and observed in the wind tunnel (Snyder and Lawson[13]). The lengths were defined as the distance from the lee wall to the point of streamline reattachment.

$$H_C = H_R\left[1-\frac{\left(x-\frac{R}{2}\right)^2}{\left(L+L_R-R\right)^2}\right]^{1/2} \qquad (R/2 < x < L_R) \tag{6}$$

Based on an analysis of horizontal-plane streamlines in wind-tunnel simulations by Snyder and Lawson[11], the horizontal cavity boundary is estimated as,

$$W_C = \frac{W}{2}+\frac{R}{3}-\frac{(x-R)^2}{3R} \qquad (0 < x \le R) \tag{7}$$

$$W_C = \left(\frac{W}{2}+\frac{R}{3}\right)\sqrt{1-\left(\frac{x-R}{L+L_R-R}\right)^2} \qquad (R < x < L+L_R) \tag{8}$$

The height of the wake boundary ($H_w(x)$) is estimated by combining the formulation of Wilson[19], based largely on measurements over the building,

$$\mathrm{H_W} = \mathrm{H} + 0.28\mathrm{R}\left[\frac{\mathrm{x}}{\mathrm{R}}\right]^{1/3} \tag{9}$$

with that of Weil[23] for the wake downwind of the building

$$H_W = 1.4H\left[\frac{\mathrm{x}}{\mathrm{H}}\right]^{1/3} \tag{10}$$

This yields,

$$H_W = 1.2R\left[\frac{x}{R}+\left(\frac{H}{1.2R}\right)^3\right]^{1/3} \tag{11}$$

For a building with H = W, Equation (11) predicts a wake height of 1.4 building heights at one building height from the upwind face and 3.3 building heights at twenty building heights from the upwind face.

The lateral boundary of the wake ($W_w(x)$) is estimated from the streamline measurements of Snyder and Lawson[13] as,

$$\mathrm{W_W} = \frac{\mathrm{W}}{2}+\frac{\mathrm{R}}{3}\left[\frac{\mathrm{x}}{\mathrm{R}}\right]^{1/3} \tag{12}$$

This formula includes the $x^{1/3}$ dependence characteristic of three-dimensional far wake growth and compares very well with the data.

Mean Streamline Slope

The model for the slope of the mean streamlines is based on the location and maximum height (H_R) of the roof-top recirculation cavity, the length of the downwind recirculation cavity (L_R) and the building length scale (R). The wind-tunnel data, in general, show that the slope of the mean streamlines can be partitioned into five regions. Figure 5 illustrates these five regions for a cubic building (H=W=L). The modeled streamlines are shown in the upper part of the figure, and those observed in the wind tunnel (Snyder and Lawson[13]) are in the lower part. The streamline slope is zero until about a distance R upwind of the building (Region A). The region of ascent upwind of and over the building (Regions B and C) shows that streamlines attain a maximum slope near the upwind face, and continue to rise to the point of maximum height of the roof-top cavity. In Region B, streamlines below about 2H/3 do not rise over the building, but rather stagnate, or deflect around the sides. A region of streamline descent (Region D) then follows to the end of the near wake, in which the slope of streamlines follows that of the upper boundary of the near wake. Beyond, in the far wake (Region E), there is a gradual decrease in the rate of streamline descent. Also, the absolute magnitude of slope at any x decreases with height above the building. The shape of the building also affects streamline slope. For example, the descent of the mean streamlines for a very wide building is not as steep as for a narrow building of the same height and length. The descent of the mean streamlines for two buildings of the same height and width is steeper for the building with the shorter length. The magnitude of the descent changes with wind direction as the projected building width and length change. Also, wind-tunnel observations of upwind slopes near the ground show that for tall buildings (H > W) only the air above the upper one-third of the building flows over the building, but for very squat buildings nearly all the air flows over the buildings.

Using these general observations, empirical relationships for the mean streamline slopes for $z \leq H$ were constructed for each region, and a height-dependent decay factor was applied for slopes at elevations above z = H: (1) a slope of zero is used for all points in Region A; (2) a parabola was fit to the streamlines below z = H in Regions B, C, and D, yielding slopes that change linearly

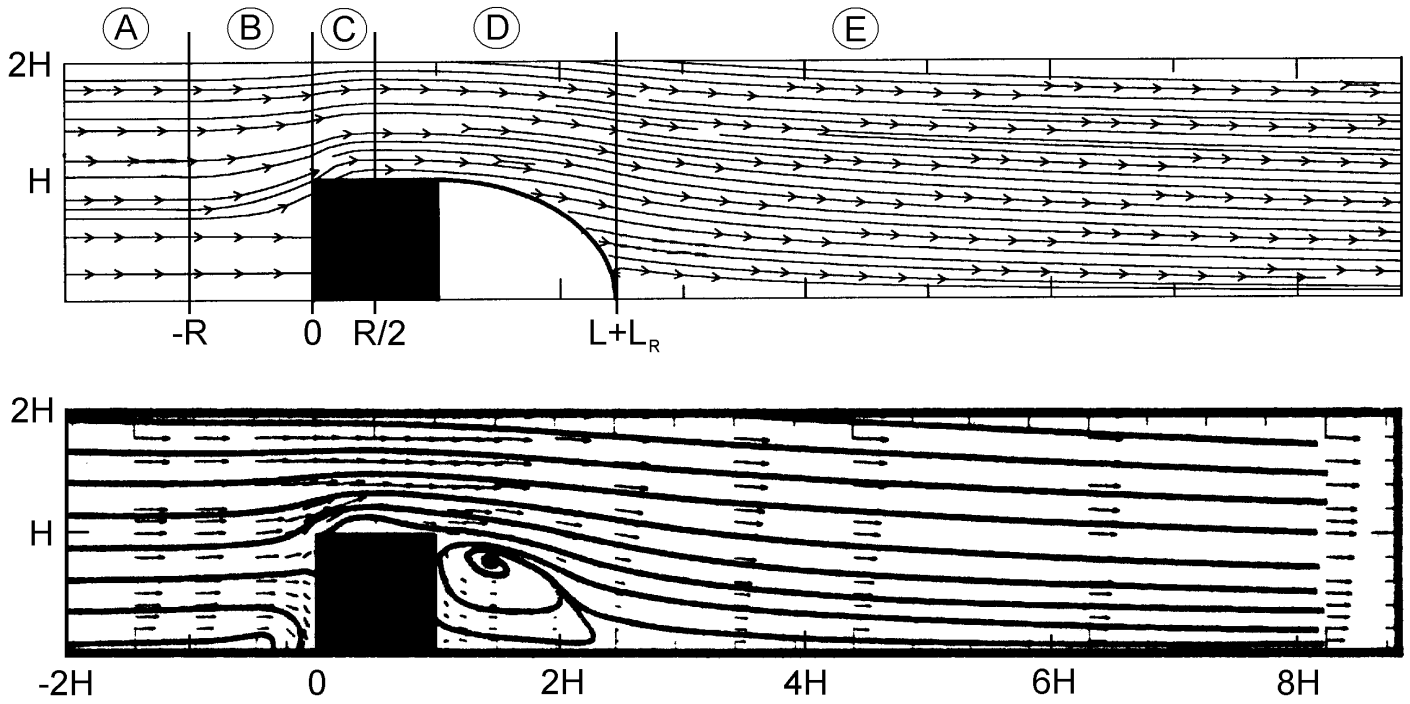

Figure 5. Comparison of streamlines predicted by the PRIME model with those observed in wind-tunnel simulations of a cubic building (Snyder and Lawson[13]). The five regions of streamline deflection (A-E) are noted. The height and distances are scaled by building height H.

with distance; the fitted streamlines rise 0.22R in both Region B and Region C, and fall 0.22R in Region D; (3) the streamline slope at the start of Region E decays as x^{-1}; and (4) slopes computed at z = H decay with z^{-3} in regions of streamline ascent and z^{-1} in regions of descent. The value of 0.22R is the maximum height of the rooftop cavity (Wilson[19]) and was found to give a good approximation to the magnitude of the deflection of the streamlines for $z \le H$. Upwind of the building (Region B), the streamline slope was maintained at zero for $z < \frac{2}{3}H$ when $R \le H$ and for $z = \frac{2}{3}(2H - R)$ when R > H. The resulting expressions for streamline slope (dz/dx) at $z \le H$ and the vertical decay factor (F_z) that is applied for z > H are:

Region	Streamline Slope	Downwind Distance from the Windward Face	Factor for z>H	
A	$\frac{dz}{dx} = 0$	$(x < -R)$	$F_z = 1$	(13)
B	$\frac{dz}{dx} = \frac{2(H_R - H)(x + R)}{R^2}$	$(-R \le x < 0)$	$F_z = \left[\frac{z}{H}\right]^{-3}$	(14)
C	$\frac{dz}{dx} = \frac{-4(H_R - H)\left(\frac{2x}{R} - 1\right)}{R}$	$(0 \le x < 0.5R)$	$F_z = \left[\frac{z}{H}\right]^{-3}$	(15)
D	$\frac{dz}{dx} = \frac{(H_R - H)(R - 2x)}{\left(L + L_R - \frac{R}{2}\right)^2}\left(\frac{z}{H}\right)^{0.3}$	$(0.5R \le x \le L + L_R)$	$F_z = \left[\frac{z}{H}\right]^{-1}$	(16)

For crosswind distances outside of the projected width of the building the slopes are linearly decreased to zero at a crosswind distance of $\frac{W}{2} + \frac{R}{3}$. This cross-stream relaxation is based on unpublished streamline plots provided by Snyder[24].

Streamline slopes predicted at z = H for several points downwind of the buildings were compared to the streamline slopes presented by Snyder and Lawson[13] for ten different building shapes. This comparison, which showed excellent agreement, was reported in Schulman and Scire[25] and is reproduced as Figure 6. The correlation coefficient from a linear fit to these data is 0.90.

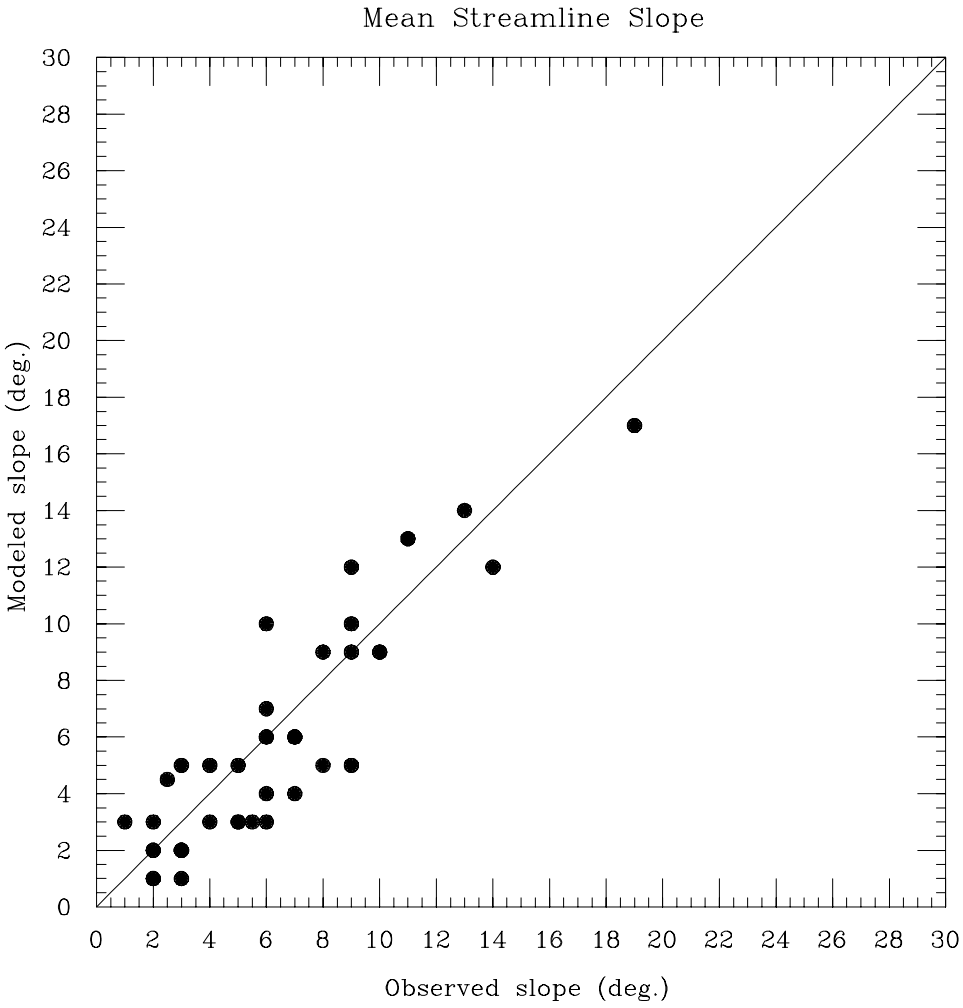

Figure 6. Comparison of the mean streamline slope for ten different building shapes as calculated by the PRIME model and observed in the wind tunnel (Snyder and Lawson[13]). The slopes were determined at building height at 3-4 points downwind of each building.

Plume Rise

The PRIME plume rise is computed using a numerical solution of the mass, energy and momentum conservation laws (Zhang and Ghoniem[26]). The model allows arbitrary ambient temperature stratification, arbitrary uni-directional wind shear, and arbitrary initial plume size. It includes radiative heat losses and can be run in a non-Boussinesq mode. The implementation of the plume rise model in PRIME allows for streamline ascent/descent effects to be considered, as well as the enhanced dilution due to building-induced turbulence. A key feature of the model is its ability to include vertical wind shear effects, which are important for many buoyant releases from short stacks. Additionally, the wind speed deficit induced by the building is modified as a function of downwind distance from the building. The deficit also leads to increased plume rise from short stacks. The temperature profile is not modified from ambient values, which is conservative during stable conditions.

The governing equations for plume rise are:

(1) Mass $$\frac{d}{ds}\left(\rho U_{sc} r^2\right) = 2r\alpha\rho_a\left|U_{sc} - U_a\cos\Phi\right| + 2r\beta\rho_a\left|U_a\sin\Phi\right| \quad (17)$$

where $\alpha = 0.11$ and $\beta = 0.6$ (Hoult and Weil [27]) are the entrainment parameters corresponding to the differences of velocity components between the wind and the plume in directions parallel and normal to the plume centerline, $U_a(z)$ is the ambient horizontal wind speed, which can be an arbitrary function of height; and

$$U_{sc} = \sqrt{u^2 + w^2} \quad (18)$$

is the velocity of the plume cross section along its centerline, with two components u and w in the horizontal and vertical directions, ρ and ρ_a are the plume density and air density, respectively, s is the distance along the plume centerline measured from the emission source, r is the plume radius, and ϕ is the centerline inclination.

(2) Momentum - Along- wind $$\frac{d}{ds}\left(\rho U_{sc} r^2 \left(u - U_a\right)\right) = r^2 \rho w \frac{dU_a}{dz} \quad (19)$$

(3) Momentum – Vertical

$$\frac{d}{ds}\left(\rho U_{sc} r^2 w\right) = g r^2 \left(\rho_a - \rho\right) \tag{20}$$

where g is the gravitational acceleration.

(4) Energy

$$\frac{d}{ds}\left[\rho U_{sc} r^2 \left(T - T_a\right)\right] = -\left[\frac{dT_a}{dz} + \frac{g}{c_p}\right]\rho w r^2 - R_p r\left(T^4 - T_a^4\right) \tag{21}$$

where T is the plume temperature, T_a is the ambient temperature, c_p is the specific heat of ambient air and R_p is a variable characterizing the radiation properties with a value of 9.1 x 10^{-11} kg/(m^2K^3s).

The effect of increased wake turbulence on entrainment is included by assuming that the mass entrainment equation (Equation (17)) may be dominated at times by the plume growth due to the wake turbulence. This is implemented by using the maximum of the two entrainment rates each step,

$$\frac{d}{ds}\left(\rho U_{sc} r^2\right) = \text{Maximum}\left(\left(\frac{d}{ds}\left(\rho U_{sc} r^2\right)\right)_{\text{entrainment}}, 2r\rho_a U_a \left(\frac{dr}{ds}\right)_{\text{wake}}\right) \tag{22}$$

The radial growth rate due to wake turbulence is obtained from the growth rate of the vertical spreading parameter σ_z, (whose formulation is discussed in the next section)

$$\left(\frac{dr}{ds}\right)_{wake} = \sqrt{\frac{\pi}{2}} \quad \frac{d\sigma_z}{dx} \tag{23}$$

For plume rise downwind of the building, the ambient wind speed profile is modified to reflect the reduced wind speeds in the wake, so that

$$U_w(z) = F(z) U_a(z) \tag{24}$$

where F(z) is the fraction of the ambient wind speed. Within the cavity, F equals a constant (F_c), and above the wake, F = 1. F is a linear function of height between H_C and H_W,

$$F = F_c + \left[\frac{1 - F_c}{H_w - H_c}\right](z - H_c) \qquad (H_c \le z \le H_w) \tag{25}$$

F_C is calculated by assuming a mean fractional velocity deficit through the full depth of the wake at the lee wall of the building, $\Delta U_0/U_0$, where U_0 is a uniform speed upwind of the building. This constraint with Equation (25) forces F_c to be,

$$F_c = 1 - \left[\frac{H_w(\Delta U_0/U_0)}{0.5(H_w + H_c)}\right] \tag{26}$$

The value of $\Delta U_0/U_0$ was estimated as 0.7 from the wind-tunnel data of Snyder and Lawson[11]. The modified wind profile in the wake was allowed to decay from the lee wall to the ambient profile with an $x^{-2/3}$ dependence, based on Weil's[23] model of the wake region.

Dispersion Coefficients

Dispersion is based on the approach of Weil[23]. Enhanced turbulence intensity and velocity deficit values are calculated within the wake region. These values are a maximum at the lee wall of the building and decay with the two-thirds power downwind. If the plume is released upwind of the wake, the plume initially grows at the ambient rate. At the point that the plume centerline intercepts the wake, a probability density function (p. d. f.) model is used for plume dispersion over a distance equal to the length of the near wake, and an eddy diffusivity model for plume growth is used beyond. The key assumption in the p.d.f. approach is that the travel time is short enough that particles released by the source remember their initial velocity. When the turbulence intensity within the wake has decayed to the ambient intensity, a virtual source technique is used to transition to the ISC3 dispersion curves. For an unstable ambient stability, or if the plume is intercepted by the wake several building heights downwind, the building effects on plume dispersion may be small and short-lived. This is consistent with the Castro and Robins[28] wind-tunnel simulation of flow around a cube for a fairly rough suburban boundary layer. They found that the wake decayed completely within about six cube heights downstream. Nearer to the building or with neutral and stable approach flows the building effects will be larger. The formulation is presented for vertical dispersion, but is analogous for the horizontal dispersion.

Following Weil[23] , who estimated constants from the wind-tunnel data of Arya and Gadiyaram[29], turbulence intensity, i_z, is calculated within the wake at a distance (ξ-R) from the lee wall (where ξ is defined such that ξ = R at the lee wall) as the quotient of the turbulence velocity in the wake and the mean wind speed in the wake,

$$i_z = \frac{\sigma_w}{U} = \frac{\sigma_{w0} + (1.7\sigma_{wN} - \sigma_{w0})\left[\frac{\xi}{R}\right]^{-\frac{2}{3}}}{U_0 - \Delta U_0\left[\frac{\xi}{R}\right]^{-\frac{2}{3}}} \quad (27)$$

where the subscript 0 denotes ambient values and σ_{wN} denotes the turbulence velocity typical of neutral flows. At the lee wall, ξ=R, the turbulence intensity is a maximum,

$$i_z = \frac{1.7\sigma_{wN}}{U_0 - \Delta U_0} = \frac{1.7 i_{zN}}{1 - \frac{\Delta U_0}{U_0}} \quad (28)$$

At large ξ/R, the ambient turbulence is recovered

$$i_z = \frac{\sigma_{w0}}{U_0} = i_{z0} \quad (29)$$

Recasting Equation (27) using turbulence intensity, and rearranging terms,

$$i_z = i_{z0}\left[1 + \frac{\left(\frac{1.7 i_{zN}}{i_{z0}} - 1\right) + \frac{\Delta U_0}{U_0}}{\left(\frac{\xi}{R}\right)^{\frac{2}{3}} - \frac{\Delta U_0}{U_0}}\right] \quad (30)$$

The $x^{-2/3}$ decay, as used in Weil[23] is based on a free wake with uniform approach flow, but gave the best agreement with wind-tunnel turbulence measurements (Snyder and Lawson[13]). Consistent with the plume rise formulation, $\Delta U_0/U_0$ was estimated as 0.7 from the wind-tunnel data. The values of 0.06 for i_{zN} and 0.08 for i_{yN} were inferred from the Briggs dispersion coefficient formula for neutral stability and rural conditions as reported in Gifford[30]. Ambient turbulence intensities for i_{z0} and i_{y0} were inferred from the Briggs dispersion coefficient formulas for rural and urban. These values led to good modeled agreement with the observed data presented later in the paper.

Within the p. d. f. growth region spanning a travel distance equal to the length of the near-wake, the change in the plume spread with distance is proportional to the local turbulence intensity, $\frac{d\sigma_z}{dx} = i_z(x)$. . An eddy diffusivity growth model is used beyond the p.d.f. region, following Weil[23], by assuming

$$\frac{d\sigma^2}{dx} = \frac{2K_z}{U} = \frac{k\sigma_w H_w}{U} = k\, i_z(x) H_w(x) \tag{31}$$

By matching the growth rate at x_d, the distance from the upwind building face to the point of transition from the p. d. f. to eddy diffusivity growth regime it can be shown that,

$$\frac{d\sigma^2}{dx} = 2\sigma_z(x_d)\, i_z(x)\, \frac{H_w(x)}{H_w(x_d)} \tag{32}$$

The eddy diffusivity growth rate is followed to the distance at which the turbulence intensity has decayed to the ambient value, or 15R from the downwind face of the building, whichever distance is smaller. The cap at 15R is needed for very stable ambient turbulence levels where the decay distance is unreasonably long. A virtual source distance is used to match the ambient dispersion coefficients for all further distances. Note that in the ISC downwash model, the transition to ambient dispersion is always made at 10H or 10W, whichever is less.

Both the horizontal and vertical dispersion coefficients are enhanced within the building wake. This is supported by Snyder and Lawson[11] and the original wind-tunnel data for Huber and Snyder[6]. This virtually eliminates the suspiciously large predictions by ISC3 during light wind speed, stable conditions which are caused by only enhancing the vertical dispersion coefficient when the stack height is more than 20% higher than the building height.

Near/Far Wake Concentrations

PRIME predicts concentrations in both the near and far wakes. The near wake concentration has a vertically mixed component resulting from the capture and recirculation of some fraction of the elevated primary plume by the near wake. From Wilson and Britter[21], this concentration is,

$$C_N = \frac{B f Q \exp\left(-\frac{1}{2}\left(\frac{y}{\sigma_{yc}}\right)^2\right)}{U_H H_c W_B'} \tag{33}$$

where f is the fraction of the plume mass captured by the near wake, Q is the emission rate, W'_B is the width scale through which the plume is mixed, σ_{yc} is the horizontal dispersion coefficient for cavity dispersion, and the constant B is taken as 3 (Wilson and Britter[21]). W'_B is nominally the building width, but with a maximum value of $3H_B$ and minimum value of $H_B/3$. Wilson and Britter had suggested 4 H_B as the maximum value, but comparisons with Thompson[31] wind-tunnel observations in the near wake led to the adopted values. In addition, for plumes released upwind of the cavity, W'_B is obtained from the plume σ_y at the lee wall using the equivalent top-hat distribution. This accounts for initial horizontal plume growth upwind of the cavity. The value σ_{yc} is calculated as $W'_B/(2\pi)^{0.5}$, which also assumes a top-hat distribution.

The fraction of the plume captured by the near wake is calculated in several steps. Using the equations for the height and width of the near wake boundary, the fractions of the vertical plume mass distribution, f_Z, and the horizontal plume mass distribution, f_Y, that are within the boundary of the near wake, are calculated at many distances along the near wake length. The fraction captured is then estimated as the maximum of the product $f_Z f_Y$ along the near wake length. This concept can be seen from Figure 2 for the vertical distribution. The plume emanating from the rooftop stack is partially intercepted by the near wake boundary. The fraction that is intercepted changes with downwind distance and can be calculated from:

$$f_z(x) = \mathrm{erf}\left(\frac{H_c(x) - H_p(x)}{\sqrt{2}\,\sigma_z(x)}\right) \tag{34}$$

where H_p is plume height. Because plumes released within the near wake would always have 100% capture with this procedure, the value of f_Z was capped at the fraction below H_B at the end of the near wake to allow plumes with momentum or buoyancy to partially or fully escape capture. The choice for the f_z cap was based upon comparisons of vertical plume profiles with the wind-tunnel data of Snyder[10].

That plume mass captured by the near wake is re-emitted to the far wake as a volume source. The volume source is modeled as a ground-level point source located at the base of the lee wall. The growth of the point source at this location is used as a surrogate for the loss of cavity mass up the wall and through the surface boundary of the cavity as it fluctuates unsteadily. This source

is only applied to the far wake using the formula,

$$C_F = \frac{fQ \exp\left(-\frac{1}{2}\left(\frac{y}{\sigma_y}\right)^2\right)}{\pi U_s \sigma_{zc} \sigma_{yc}} \tag{35}$$

where σ_y has the initial value σ_{yc} at the lee wall and σ_z has the initial value σ_{zc}, which is calculated by matching C_N=C_F at the lee wall. σ_{yc} and σ_{zc} grow using the same methods as for the elevated plume.

Also contributing to the far wake is the portion of the primary plume that is not captured by the near wake. This second source has mass rate (1-f) Q and follows the Gaussian plume formulation to calculate the concentration C_p,

$$C_p = \frac{(1-f)Q \exp\left(-\frac{1}{2}\left(\frac{H_p}{\sigma_z}\right)^2\right) \exp\left(-\frac{1}{2}\left(\frac{y}{\sigma_y}\right)^2\right)}{\pi \sigma_y \sigma_z U_s} \tag{36}$$

The terms for receptors above ground level and for reflection from the top of the mixed layer are not shown, but these terms are identical to those in the ISC model.

A transition zone between the near and far wakes is used to represent the unsteadiness of the near wake/far wake interface, and based on observations of the fluctuations of reattachment lengths in wind tunnels by Hosker[1], is taken as the region within 15% of the mean interface location. In the transition zone, a linear interpolation using a weighting parameter λ is made from the near wake, C_N, to far wake, C_F, concentrations. C_P is added beyond the end of the near wake to calculate the total concentration.

In summary, for the near and far wake concentrations,

$$C=C_n \qquad (L \leq x \leq L+0.85\ L_R) \tag{37}$$

$$C=\lambda C_N + (1-\lambda)C_F \qquad (L + 0.85L_R \leq x < L+L_R) \tag{38}$$

$$C=C_p + \lambda C_N +(1-\lambda)C_F \qquad (L + L_R \leq x \leq L + 1.15\ L_R) \qquad (39)$$

$$C=C_p + C_F \qquad (x \geq L + 1.15\ L_R) \qquad (40)$$

where λ decreases linearly from $\lambda = 1$ at $x = L + 0.85L_R$ to $\lambda = 0$ at $x = L + 1.15L_R$.

COMPARISON WITH OBSERVATIONS

Snyder Wind-Tunnel Data

As reported earlier, a portion of the wind-tunnel data collected for this effort, Snyder[10], included systematic variations of stack to building height ratios, ratios of exhaust speeds to wind speeds, wind angle, Froude number and stack location for both a generic steam boiler and combustion turbine. Figure 7 shows the comparison of PRIME and ISC3 predicted concentrations with observations at 15 building heights downwind for the steam boiler. The building width is twice the height and 2.5 times the length. The stack is located in the middle of the wider horizontal dimension and is 1.5 times the building height. The stack is downwind of the building for a direction of zero degrees, which is defined as perpendicular to the wider horizontal dimension. Five different wind angles to the building face were simulated in the tunnel. For all of these cases, the plume has an exhaust speed to wind speed ratio of 1.5 and a Froude number of 16. This is a highly buoyant plume with a full-scale equivalent buoyancy flux of 528 m^4/s^3.

PRIME better matches the concentration trends with wind direction. The lowest concentrations are both observed and predicted with winds perpendicular to the shorter dimension. For this direction, the stack is along the side of the building halfway down the length. The wake will have smaller dimensions for this case. For both the 45 degree and 135 degree cases, the wind is at a 45 degree angle with the larger horizontal dimension, but the stack is upwind of the building for the 135 degree case, resulting in slightly lower concentrations. The concentrations for these cases is a competition between the plume height, which is higher for the 135 degree case and the plume dimensions, which are larger for the 45 degree case.

ISC3 not only underestimates the observed concentrations for all cases except for the 90-degree direction, but also shows almost no variation with wind direction. This is because the projected

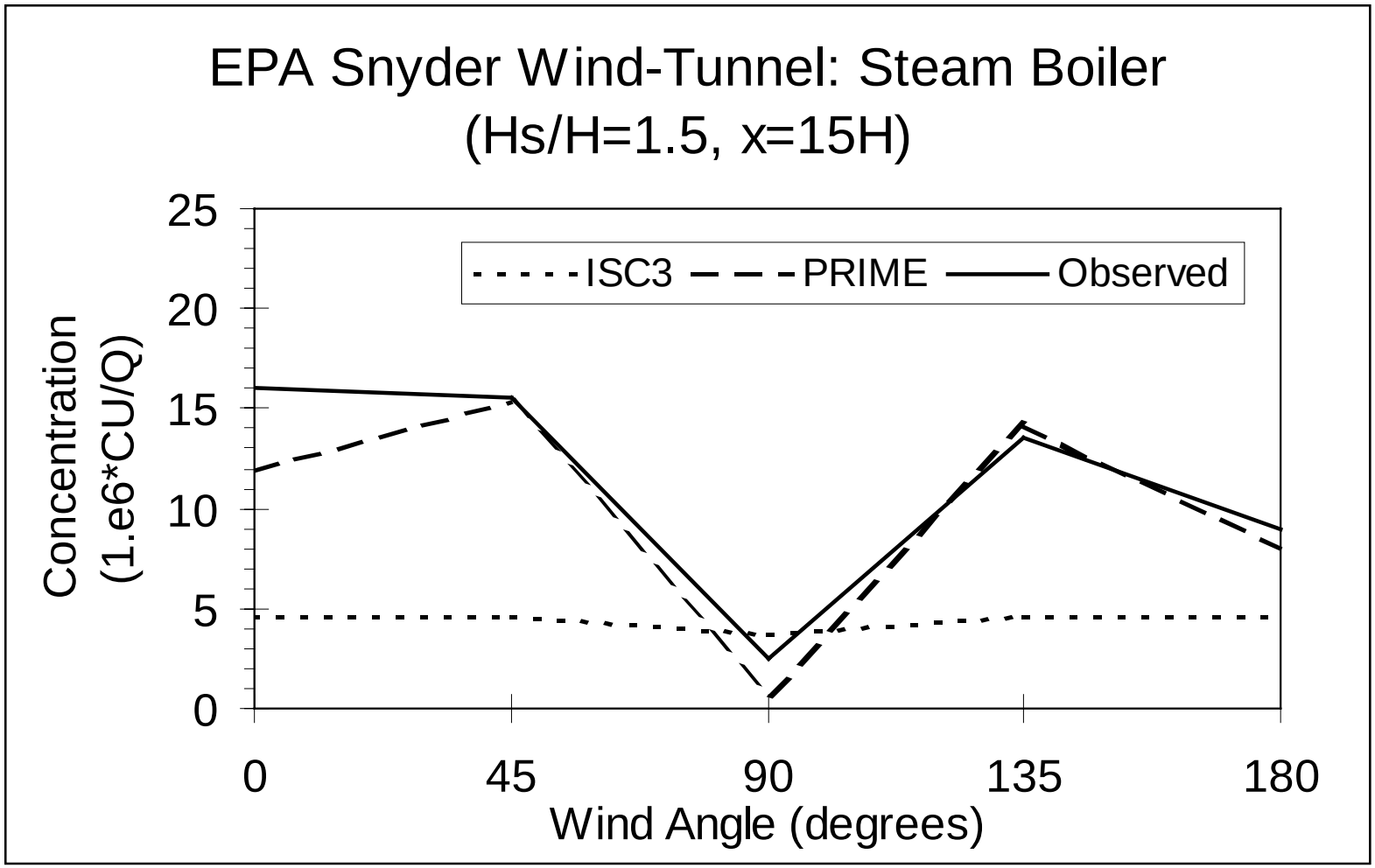

Figure 7. Comparison of concentrations predicted by the PRIME and ISC3 models with those observed in wind-tunnel simulations of emissions from a steam boiler (Snyder[10]). The concentrations are at a distance of 15 building heights downwind for five different wind angles. The vertical axis is concentration normalized by wind speed and emission rate.

width is larger than the building height for all but the 90-degree direction. The vertical dispersion coefficient in ISC3 only depends on projected width when the building height is larger than the projected width. Plume trajectory, wind speed and the horizontal dispersion coefficient are always unchanged with wind direction in ISC3 for this stack height.

Thompson Wind-Tunnel Data

These data[31] consist of non-buoyant, zero-momentum releases upwind of and in the near and far wakes of four different building shapes. Concentrations were measured at ground level on the centerplane. Figure 8 shows the comparison of PRIME and ISC3 predicted concentrations with observed concentrations for a source in the downwind cavity of a cubic building. The source is one building height downwind of the lee wall and half the building height above the ground. The flow is perpendicular to the building. Because ISC3 is only valid beyond three building heights downwind, SCREEN3 was used to predict the cavity concentration. In this case the ISC3 predictions are not valid until four building heights from the lee wall, since the building is moved to the source location in ISC3.

As can be seen in Figure 8, when a passive source is released in the cavity, the concentrations are not uniform. The peak concentration is observed at the downwind location of the source and some mass is mixed upwind. PRIME agrees reasonably well with observations in the cavity, underestimating the peak value by about 25%, but overestimating about half the cavity concentrations. Beyond the cavity, which extends less than two building heights downwind from the lee wall, PRIME shows very good agreement with observations.

SCREEN3 underestimated all the cavity concentrations, including the peak value by about 65%. The ISC3 predictions, which start at four building heights downwind, do as well as PRIME with the observations.

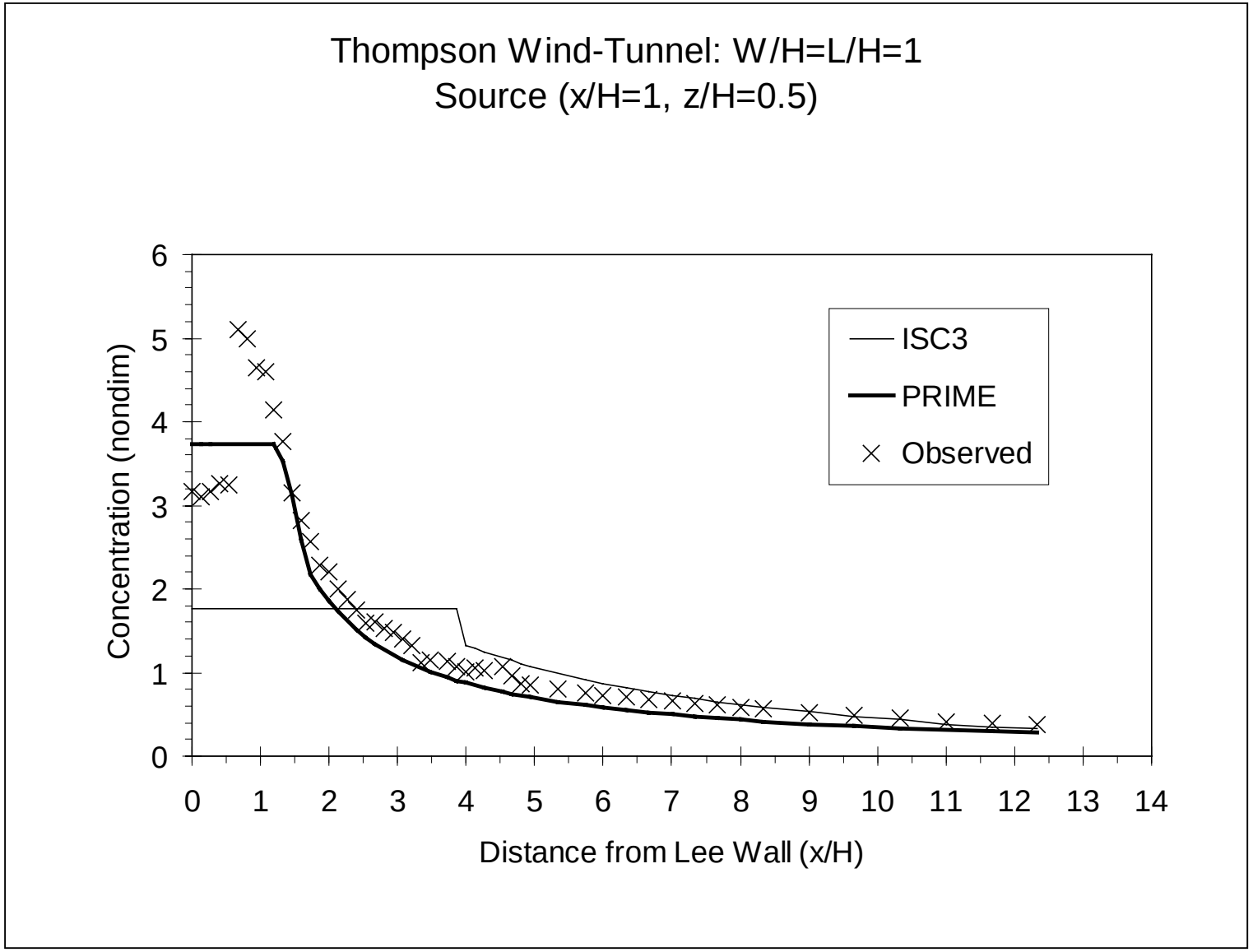

Figure 8. Comparison of concentrations predicted by the PRIME and ISC3 models with those observed in wind-tunnel simulations of a source located in the downwind recirculation cavity of a cubic building (Thompson[31]). The vertical axis is non- dimensional concentration and the horizontal axis is distance from the lee wall in building heights, H.

Alaska North Slope Field Study

A field study was conducted near Prudhoe Bay (Guenther, Lamb and Allwine[32]) for a high buoyancy, high momentum combustion turbine with a stack to building height ratio of 1.15. The buoyancy flux was 355 m^4/s^3 and the momentum flux 575 m^4/s^2. Thirty-eight hours of SF_6 tracer data and onsite meteorological data were collected during very high wind speed conditions (up to 18 m/s) over a 7 day period. Samplers were placed at up to 60 locations, in arcs at distances from 20 m to 3400 m, so that the largest concentrations could be measured.

Figure 9 shows a quantile-quantile plot of the maximum observed and predicted concentrations for each of the 38 hours. Hour-by-hour comparisons are often not meaningful because of the uncertainties in meteorological conditions and model components. For the largest observed concentrations PRIME shows much better agreement than ISC3. PRIME overestimates the largest concentration by 31%, while ISC3 overestimates by 296%. Both models overestimate the smaller observed concentrations, but PRIME overestimates by a smaller margin. For the highest predicted concentrations, PRIME estimates lower plume heights than ISC3, but also smaller dispersion coefficients.

Bowline Point Power Plant

One-half year of measured meteorological, emissions and concentration data for a 1200 MW power plant (Schulman and Hanna[8]) were used to evaluate ISC3 and PRIME. The plant has two identical stacks that are 1.33 times the building height of 65.2 m. Only two monitors observed any significant concentrations. The highest concentrations were observed at a monitor 848 m from the midpoint of the stacks during hours with high wind speeds. Meteorological data were measured at a 100 m tower located 250 m from the plant.

Figure 10 shows the ten highest observed and predicted concentrations at the monitor with the largest observed values, as well as the stability class associated with that hour. These values are unpaired in time. PRIME is within 3% of each of the top three observed concentrations and overestimates the tenth highest value by 29%. ISC3 overestimates the highest three observations by an average of 21% and the tenth highest value by 40%.

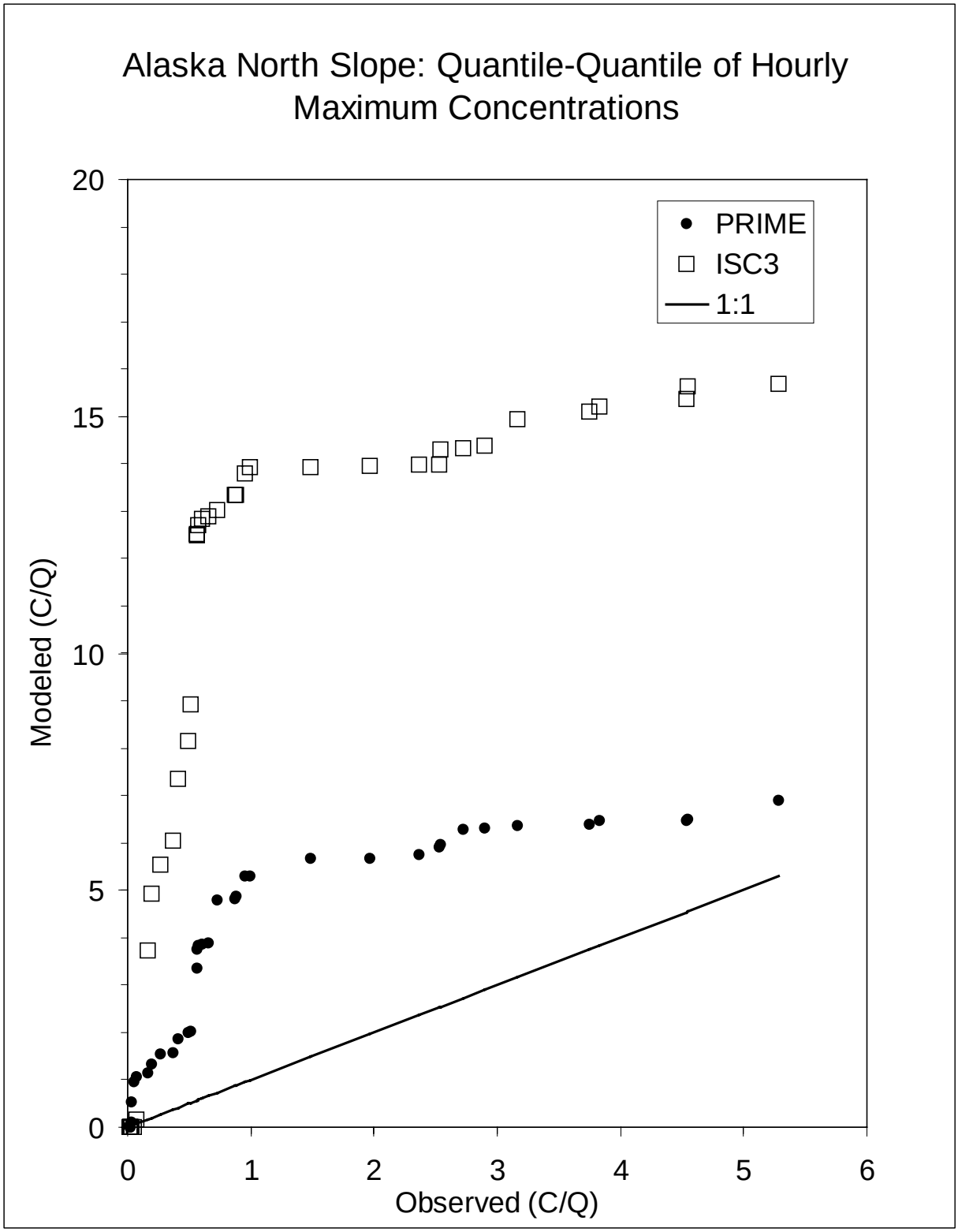

Figure 9. Ranked comparison of the maximum concentrations (normalized by emission rate) predicted by PRIME and ISC3 with the highest concentrations observed during each of the 38 hours of a field study on the Alaska North Slope (Guenther, Lamb and Allwine[32]). The source was a highly buoyant combustion turbine.

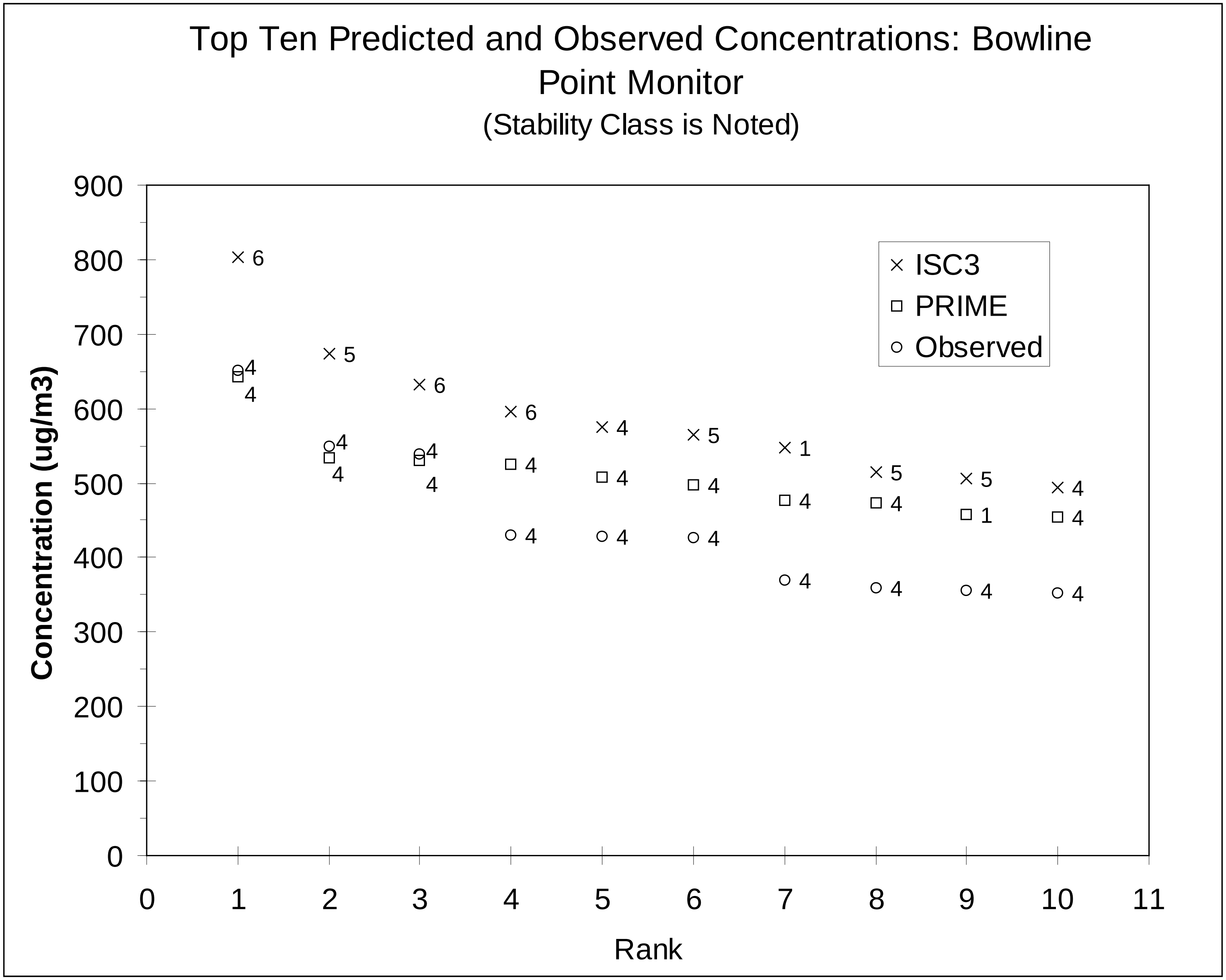

Figure 10. Comparison of the ten highest hourly concentrations predicted by the PRIME and ISC3 models with those observed at a monitor near the Bowline Point Generating Station. The atmospheric stability class associated with each concentration is noted (1=very unstable, 2=unstable, 3=slightly unstable, 4=neutral, 5=slightly stable and 6=stable).

PRIME correctly matches the high wind speed, neutral stability conditions (stability class 4) of the highest observed hours. In fact, four of the highest concentrations predicted by PRIME occur during the same hours as the ten highest observed values. All of the ten highest observations are during neutral stability conditions and nine of the ten highest concentrations predicted by PRIME occur during neutral stability conditions. Only one of the ten highest concentrations predicted by ISC3 occurs during an hour with one of the ten highest observed concentrations. Seven of the ten highest are predicted to occur during stable conditions. Much lower concentrations were actually measured during hours with stable conditions.

CONCLUSIONS

The PRIME model includes several advances in modeling building downwash effects including enhanced dispersion in the wake, reduced plume rise due to streamline deflection and increased turbulence, and a continuous treatment of the near and far wakes. All of these effects consider the location of the plume within the wake. Comparisons of the model with wind-tunnel and field data have shown improved performance over the current ISC3 model. The PRIME model is implemented within the ISC3 model code, but can be implemented in other refined or screening air quality models.

ACKNOWLEDGMENTS

This research was sponsored by EPRI of Palo Alto, CA and participating EPRI members. The authors are thankful for the support of Dr. Charles Hakkarinen, the EPRI project manager, Richard Osa of Science and Technology Management, the project administrator, Richard Dunk of Jersey Central Power and Light for providing the field study facility, Dr. William Snyder of NOAA, Roger Thompson of EPA, and Dr. William Melbourne of Monash University for providing wind tunnel data, and Dr. Rex Britter of the University of Cambridge, project consultant, for his helpful discussions.

NOMENCLATURE

α	entrainment parameter parallel to the plume centerline
β	entrainment parameter normal to the plume centerline
B	empirical constant (recirculation factor for near wake concentration)
B_L	larger of H and W
B_S	smaller of H and W
C_F	contribution to the far wake concentration from fraction of the plume captured by the near wake ($\mu g\ m^{-3}$)
C_N	near wake concentration from fraction of the plume captured by the near wake ($\mu g\ m^{-3}$)
c_P	specific heat of ambient air ($J\ kg^{-1}\ K^{-1}$)
C_P	contribution to the far wake concentration from portion of the plume not captured by the near wake ($\mu g\ m^{-3}$)
dz/dx	mean streamline slope
F	fraction of the ambient wind speed at height z in wake
f	fraction of the plume mass captured by the near wake
F_C	constant value of F in the cavity
f_Y	fraction of the horizontal plume mass captured by the near wake
F_Z	vertical decay factor for streamline slope for z>H
f_Z	fraction of the vertical plume mass captured by the near wake
g	acceleration of gravity ($m\ s^{-2}$)
H	building height (m)
H_C	height of the downwind recirculation cavity (m)
H_P	plume height (m)
H_R	maximum height of the downwind recirculation cavity (m)
H_W	height of the wake boundary (m)
i_z	vertical turbulence intensity
i_{zN}	value of i_z typical of neutral flow
i_{z0}	ambient value of i_z
L	projected building length along the flow (m)
λ	linear weighting factor (from 0 to 1) for contributions from C_N and C_F in the transition zone between the near and far wakes
L_R	distance along the downwind recirculation cavity measured from lee face (m)
ϕ	angle of plume centerline inclination with the horizontal (rad)
Q	emission rate ($g\ s^{-1}$)
R	building length scale (m)
r	plume radius (m)
ρ	density of plume ($kg\ m^{-3}$)
ρ_a	density of ambient air ($kg\ m^{-3}$)
R_P	plume radiation properties with value 9.1×10^{-11} $kg\ m^{-2}\ K^3\ s$ if emissivity is taken as 0.8
s	distance along the plume centerline measured from the emission source (m)
σ_w	standard deviation of the turbulent velocity fluctuations in the vertical ($m\ s^{-1}$)

σ_{w0} ambient value of σ_w (m s^{-1})

σ_{wN} value of σ_w typical of neutral flow (m s^{-1})

σ_y standard deviation of the lateral concentration distribution, referred to as the horizontal dispersion coefficient (m)

σ_{yc} horizontal dispersion coefficient for the downwind recirculation cavity (m)

σ_z standard deviation of vertical concentration distribution, referred to as the vertical dispersion coefficient (m)

σ_{zc} vertical dispersion coefficient for the downwind recirculation cavity (m)

T plume temperature (K)

T_a ambient temperature (K)

u along-wind velocity component (m s^{-1})

U_a ambient wind speed (m s^{-1})

U_H ambient wind speed at building height (m s^{-1})

U_0 uniform wind speed upwind of the building used as part of ratio $\Delta U_0/U_0$

U_{SC} velocity of the plume along centerline (m s^{-1})

U_w wind speed in the wake (m s^{-1})

W projected building width across the flow (m)

w vertical velocity component (m s^{-1})

W'_B building width scale through which plume is mixed in the recirculation cavity (m)

W_C width of the downwind recirculation cavity (m)

W_W width of the wake boundary (m)

x along-wind distance measured from the upwind face of the building (m)

ξ downwind distance defined so that it equals R at the lee wall (m)

REFERENCES

1. Hosker, R. P. Jr. In *Atmospheric Science and Power Production*; D. Randerson, Ed.; DOE/TIC-27601; United States Department of Energy: Washington, DC, 1984; Chapter 7.

2. Meroney, R. N. In *Engineering Meteorology;* E.J. Plate, Ed.; Elsevier Scientific Publishing Co.: Amsterdam, 1982; pp 481-525.

3. *Screening Procedures for Estimating the Air Quality Impact of Stationary Sources - Revised* 454/R-92-019; U.S. Environmental Protection Agency: Research Triangle Park, NC, 1992.

4. *User's Guide for the Industrial Source Complex (ISC3) Dispersion Models* 454/B-95-003b; U.S. Environmental Protection Agency: Research Triangle Park, NC, 1995.

5. Schulman, L.L.; Scire, J.S. *J. Air and Waste Management Association* 1993, 43, 1122-1127.

6. Huber, A. H.; Snyder, W.H. *Atmospheric Environment* 1982, 176, 2837-2848.

7. Scire, J. S.; Schulman, L.L. In *Second Joint Conference on Applications of Air Pollution Meteorology;* American Meteorological Society: Boston, MA, 1980; pp 133-139.

8. Schulman, L.L.; Hanna, S.R. *J. Air Pollution Control Association* 1986, 36, 258-264.

9. EPRI. *Results of the Independent Evaluation of ISCST3 and ISC-PRIME*. Report TR-2460026. Palo Alto, CA, 1997.

10. Snyder, W. H. *Wind-Tunnel Simulation of Building Downwash from Electric-Power Generating Stations. Part I: Boundary Layer and Concentration Measurements*. U.S. Environmental Protection Agency: Research Triangle Park, NC, 1992.

11. Snyder, W.H., Lawson, R. *Wind-Tunnel Simulation of Building Downwash from Electric-Power Generating Stations. Part II: Pulsed-Wire Measurements in Vicinity of Steam-Boiler Building*. U.S. Environmental Protection Agency: Research Triangle Park, NC, 1993.

12. Snyder, W.H. In *NATO Advanced Research Workshop, Recent Advances in the Fluid Mechanics of Turbulent Jets and Plumes;* Viano so Castelo, Portugal, 1993.

13. Snyder, W.H.; Lawson, Jr., R.E. In *Eighth Joint Conference on Applications of Air Pollution Meteorology with A&WMA*; American Meteorological Society: Boston, MA, 1994; pp 244-250.

14. Melbourne, W. H.; Taylor, T.J. *Plume Rise and Downwash Wind Tunnel Studies: Combustion Turbine Unit 4 Sayreville; Draft Final Report*; Monash University Department of Mechanical Engineering: Clayton, Victoria, Australia, 1994; TR-235274.

15. Oncley, S. *Summary of ASTER Operations During DOWNWASH94, Final Report;* National Center for Atmospheric Research: Boulder, CO, 1994.

16. Kaiser, R. D.; Nielsen, N.; Uthe, E. *Remote Sensing of Plume Diffusion and Building Wake Effects. Final Report*; SRI International: Menlo Park, CA, 1994; SRI Project 50067.

17. Scire, J. S.; Schulman, L.L.; Strimaitis, D.G. In *88th Annual Meeting of the Air and Waste Management Association;* Air and Waste Management Association: Pittsburgh, PA, 1995; Paper 95-WP75B.01.

18. Brzoska, M. A.; Stock, D.; Lamb, B. In *Ninth Joint Conference on Applications of Air Pollution Meteorology with A&WMA*; American Meteorological Society: Boston, MA, 1996; pp 322-328.

19. Wilson, D. J. *ASHRAE Transactions* 1979, 85**,** 284-295.

20. *1997 ASHRAE Handbook - Fundamentals*; American Society of Heating, Refrigerating and Air-Conditioning Engineers: Atlanta, GA, 1997.

21. Wilson, D. J.; Britter, R.E. *Atmospheric Environment* 1982,16**,** 2631-2646.

22. Fackrell, J.E. *J. Wind Engineering and Industrial Aerodynamics* 1984, 16, 97-118.

23. Weil, J. C. In *Ninth Joint Conference on Applications of Air Pollution Meteorology with A&WMA*; American Meteorological Society: Boston, MA, 1996; pp 333-337.

24. Snyder, W.H., personal communication, 1995

25. Schulman, L.L.; Scire, J.S. In *Ninth Joint Conference on Applications of Air Pollution Meteorology with A&WMA*; American Meteorological Society: Boston, MA, 1996; pp 307-310.

26. Zhang, X.; Ghoniem, A.F. *Atmospheric Environment* 1993, 15, 2295-2311.

27. Hoult, D.P.; Weil, J.C., *Atmospheric Environment.* 1972, 6, 513-531

28. Castro, I. P.; Robins, A.G. *J. Fluid Mechanics* 1977, 79, 307-335.

29. Arya, S.P.S., Gadiyaram, P.S., *Atmospheric Environment* 1986, 20, 729-740

30. Gifford, F. A. *Nuclear Safety* 1976, 17, 68-86.

31. Thompson, R.S. *Atmospheric Environment* 1993, 15, 2313-2325.

32. Guenther, A.; Lamb, B.; Allwine, E. *Atmospheric Environment* 1989, 24A, 2329-2347.